Optimization of thin film growth: Materials for energy storage and conversion

A. Rougier*, Y. Makirnura, N. Penin, X. Darok and J.-M. Tarascon
Laboratoire de Réactivité et de Chimie des Solides, CNRS UMR-600 7, Université de Picardie Jules Verne, 80039 Amiens Cedex, France.

Through three examples taken in the field of energy storage and conversion, this paper reports how the property of thin films can be optimized by tuning the growth conditions. Focusing on the influence of the film composition, the substrate temperature and the pressure, oxides, fluorides, metal and hydrides thin films were successfully grown using the Pulsed Laser Deposition technique. A careful screening among a large range of metal addition (M=Co, Ta, W<20 %) enables the determination of the Ta and W compositions leading to the highest cycling stability of electrochromic Ni-based oxide thin films cycled in KOH electrolyte. The optical properties of Mg thin films are strongly sensitive to the chamber pressure as shiny metallic and transparent films are deposited in vacuum and under an Ar/H_2 mixture, respectively. Optical changes were also achieved by *ex situ* hydrogenation of Mg-C_X films. Finally, the benefit of enlarging substrate temperatures to negative values is illustrated through the example of FeF_x thin films, for which the substrate temperature is a key factor governing the FeF_2 or/and FeF_3 phase deposition.

Keywords : Pulsed Laser Deposition, Thin films, Growth Conditions

I. INTRODUCTION

Since its first use in the early sixties, the Pulsed Laser Deposition technique has rapidly emerged as a relatively simple and flexible technique allowing the growth of multi-element films from a single target **[1-2]**. Thin films with tuned characteristics such as crystallinity, texture, and stoichiometry, are indeed easily prepared by an acute control of the deposition conditions, such as laser energy, pulse duration, substrate temperature, atmosphere and so forth… In our group focusing on materials in the field of energy storage and conversion, the advantages of this technique have been largely illustrated **[3-4]**. For instance, a careful optimization of the oxygen pressure and substrate temperature allowed the growth of oxidic thin films showing promising electrochromic properties **[5]**. Herein further improvements in the electrochromic properties of NiO-based thin films will be reported in terms of film composition. Through the example of Mg-based thin films, which have in the past ten years received a strong interest as switchable mirrors due to their optical changes upon hydrogenation **[6-7]**, the importance of the pressure inside the chamber, during the thin film growth, will be emphasized. Finally, the range of materials will be extended to the characterization of transition metal fluorides, used as electrode materials in lithium batteries, for which the key role played by the substrate temperature will be discussed.

II. EXPERIMENTAL

All thin films were grown using the Pulsed Laser Deposition technique with a KrF excimer laser beam (Lambda Physic Compex 102, λ=248 nm) and a laser fluence of 1-2 $J.cm^{-2}$. For reactive systems, namely FeF_X and Mg-based thin films, to prevent air exposure upon handling and characterization, the PLD chamber was equipped with a glove box. The film structure and crystallinity were examined by X-ray diffraction (XRD) using a Philips diffractometer (θ-2θ configuration and $\lambda(Cu K\alpha)$ = 1.5418 Å). The thickness of the films was determined with a Dektak profilometer. From now on, each system will be described separately.

A - Ni-M-O

The NiO and Ni-M-O (2, 5, 10, 20 % of M (M = W, Co, Ta)) thin films were grown on FTO (i.e., SnO_2:F) coated glass substrate for 10 min to 1 h, in optimized conditions, namely at room temperature (RT) and in a 10^{-1} mbar oxygen pressure, using a repetition rate of 5 Hz. To determine their cycling life, Ni-M-O thin films were typically characterized by cyclic voltammetry in the -0.20 to 0.70 V potential window versus HgO/Hg reference electrode using a three-electrode cell configuration of conventional design filled with an aqueous molar solution of potassium hydroxide (V~20 mL). A large platinum foil was used as counter electrode. The experiments were performed on a VMP automatic cycling/data recording system (Biologic S.A., Claix, France).

B - Mg-based thin films

Mg-based thin films were grown on 1×1 cm^2 glass substrates for 10 min to 1 h at room temperature either in vacuum ($\approx 10^{-7}$ mbar) or under an Argon/Hydrogen (93/7 %) gas mixture in the 10^{-1} to 5.10^{-1} mbar range (so-called *in situ* hydrogenated film), using a 10 Hz

repetition rate. *Ex situ* hydrogenation was carried out by annealing as-deposited metallic films at 200 °C in 15 bars of hydrogen for durations lasting from 30 min to 12 h. A Varian Cary-SE double beam UV-VIS-NIR spectrophotometer was used to measure the optical transmittance in the 300 to 2500 nm range.

C - FeF

Iron fluoride thin films were grown on stainless steel substrates, for 10 min to 1 h, from high purity FeF_3 target in vacuum (5.10^{-7} mbar) using a repetition rate of 10 Hz. In the classical configuration, the substrate temperature varied from RT to 600 °C. To achieve low substrate temperature depositions, we designed a specificubstrate holder, cooled down through metallic tubes by refrigerated ethanol flowing from a cryogenic device equipped with a regulator of temperature (Vasse Julabo FP50). Substrate temperatures as low as -50 °C were successfully achieved by decreasing the laser energy to 120 mJ as a 180 mJ energy (used for RT and 600 °C) produced heat inside the chamber limiting the substrate temperature to -20 °C. The electrochemical behavior of FeF_x thin films as positive electrode in lithium cell was characterized in standard 2035-size coin cells, using a lithium foil and 1 M $LiPF_6$ dissolved in ethylene carbonate (EC)/ dimethyl carbonate (DMC) solution (1/1 by volume) as negative electrode and electrolyte, respectively. Galvanostatic measurements were carried out at a current density of 2.82 $\mu A \cdot cm^{-2}$ in a voltage window of 0.05- 3.60 V using a MacPile controller.

III. RESULTS AND DISCUSSION

A - Ni-M-O thin films : key role of the composition

Independently of the M nature, the thinnest Ni-M-O thin films are dense whereas the thickest films consist of agglomerates of few hundreds nanometers. NiO thin films deposited at RT and in 10^{-1} mbar oxygen pressure are crystallized (Fig. 1). X-ray diffraction peaks were indexed as (111), (200) and (220) using a NiO rock-salt cubic structure with a strong [111] preferred orientation. Whatever the metal nature, the M addition is associated with a loss of the [111] preferred orientation. Besides, for high Ta and W content (>5%), their presence is correlated with a rapid film amorphization. On the contrary for the Ni-Co-O system, the (002) peak remains clearly visible. As shown earlier, among all the Ni-M-O systems (M<20 %), the compositions leading to the best electrochromic performances are the Ni-W-O (W, 5%), Ni-Co- O (Co, 5 %) and Ni-Ta-O (Ta, 10 %) ones **[8-9]**. The cycling life (represented by the evolution of the coulometric capacity vs. the cycle number) of Ni-M-O thin films are typically based on a three-step process, namely the activation period (I, increase in capacity), the steady state (II, maximum of capacity) and the degradation period (III, decrease in capacity). If the W addition does not modify the length of the activation period with a maximum of the coulometric capacity reached after 100 cycles, the Co and Ta addition shift the steady state to higher cycle numbers (i.e.≈240 cycles) (Fig. 2a). Simultaneously, the M addition induces a shift of the cyclic voltammograms towards lower potential (Fig. 2b). Overall cyclic voltammograms are mainly characterized by a peak in oxidation and one in reduction, generally ascribed to the faradic process involving the Ni(II)/Ni(III) couple. Obviously, the strong increase in current at the end of the anodic sweep corresponds to the electrolyte decomposition. Ni-W-O (W, 5 %) thin films exhibit the highest capacity (Fig. 2a) whereas Ni-Ta-O (Ta, 10 %) shows the highest stability with a relative capacity close to 42 % after 4000 cycles as compared to 30 % for NiO (Fig. 2c). Moreover, the higher stability of Ni-M-O thin films is even more pronounced for smaller cycle numbers. As detailed elsewhere, such increase in stability was correlated to limited dissolution of the oxidized phases upon cycling for Ni-M-O systems (M=Ta (10 %), W (5 %)) **[9]**.

B - g-based thin films: Key rote of the atmosphere of deposition

Shiny metallic Mg films deposited in vacuum were crystallized with a [002] preferred orientation (S.G.: *P*63*/mmc* **[10]**) whereas amorphous *in situ* hydrogenated films (deposited in an Ar / H_2 gas mixture) were transparent with

an optical transmittance close to 90 % in the visible region. Not surprisingly due to the limited vacuum of our PLD set-up (P i0 mbar), HRTEM studies reveal the existence of Mg together with MgO, indicating the extreme reactivity of Mg films towards oxygen, further limiting the hydrogenation process [10].

Indeed, *ex situ* hydrogenated films exhibit an optical transmittance below 20 % in the visible region. Based on our earlier work on powder showing a decrease in oxygen content in ball-milled magnesium-based alloys and carbon composites [11], the hydrogen sorption properties of Mg-C films were investigated.

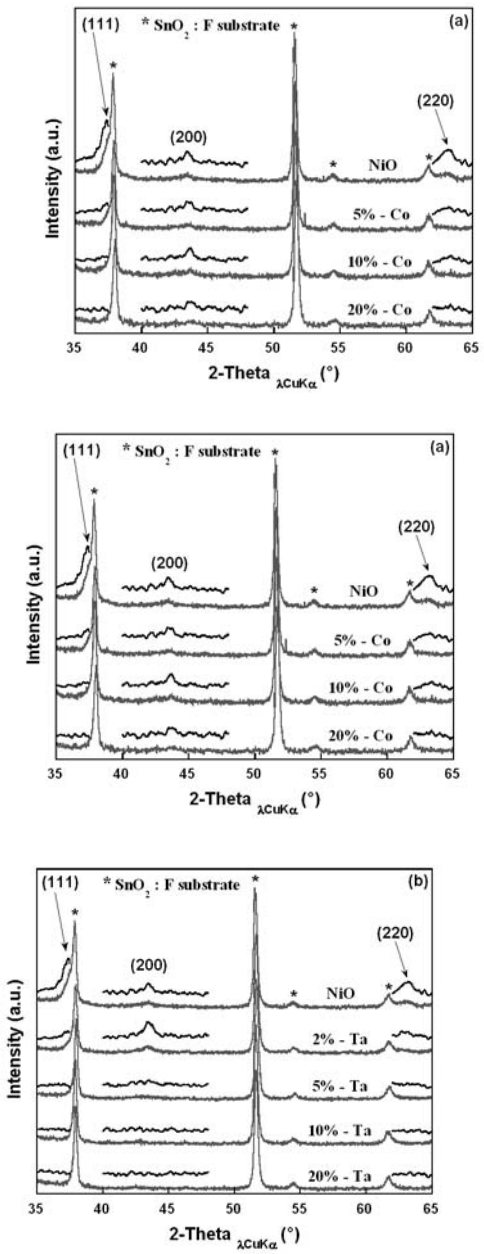

FIGURE 1 : X-ray diffraction patterns of 300 nm Ni-M-O thin films (M = Co (a), M = Ta (b), M = W (c)) deposited on Sn02:F (FTO)-coated glass substrate under 101 mbar oxygen pressure at room temperature. Difference in XRD patterns between thin films and substrate are shown at the locations corresponding to NiO peaks. The diffractograms are indexed using a NiO rock-salt cubic structure (S.G. Fm3m).

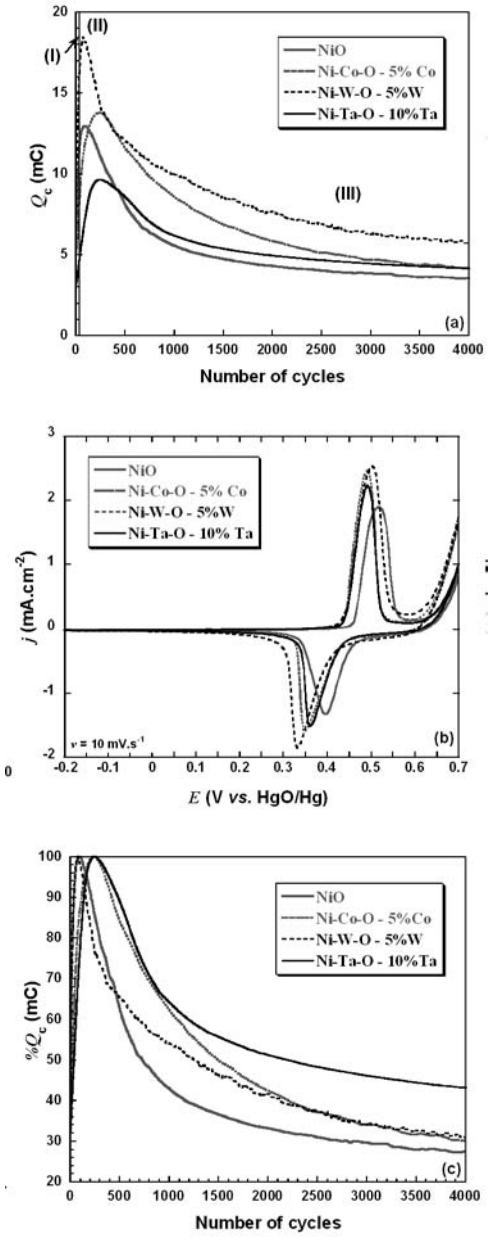

FIGURE 2 : Evolution of (a) the cathodic coulometric capacities Q and (c) the relative cathodic coulometric capacities %Q versus the number of cycles for NiO and Ni-M-O thin films (M = Co (5%), M = Ta (10%), M = W (5 %)) deposited under 101 mbar oxygen pressure at room temperature for 10 min. (b) Corresponding cyclic voltammograms recorded in the steady state (i.e. maximum capacity).

Mg-C (x weight % ≤20%) thin films were grown from Mg+x$C_{(10,320)}$ (x≤20 %) targets prepared from a mixture of Mg and 10 h pre-ball milled high surface area MCMB carbon (320 m^2/g), ball milled for 2 h. Interestingly, during the Mg-C films deposition, after each laser pulse, an increase in the pressure inside the chamber, which intensity increases with the carbon content, is observed (Table 1). This trend may

Table 1 : Evolution of the pressure inside the chamber after each laser pulse as a function of the amount of carbon inside the target for Mg-Cg thin films.

	Mg	Mg-C_5	Mg-C_{10}	Mg-C_{20}
Pressure after each laser pulse (mbar)	10^{-7}	$4\ 10^{-7}$	$7\ 10^{-7}$	2.510^{-6}

be interpreted assuming that the carbon atoms, ejected from the target, react with the residual oxygen present at 10^{-7} mbar creating carbon oxide species CO_w that increase the pressure inside the chamber. As a matter of fact, HRTEM micrographs and corresponding SAED pattern of Mg-C_x films show the presence of Mg without any traces of crystallized MgO. The oxygen content in the films was roughly estimated from EDS analyses by arbitrarily fixing the Mg counts to 2500. Their decrease from 600 to 200 counts for Mg (50 nm) and Mg- C_{10} (50 nm) confirms that less oxygen is present in the carbon containing film, respectively. A similar decrease in oxygen content with carbon addition was measured for the *in situ* hydrogenated films. However, the high value of the Ar/H_2

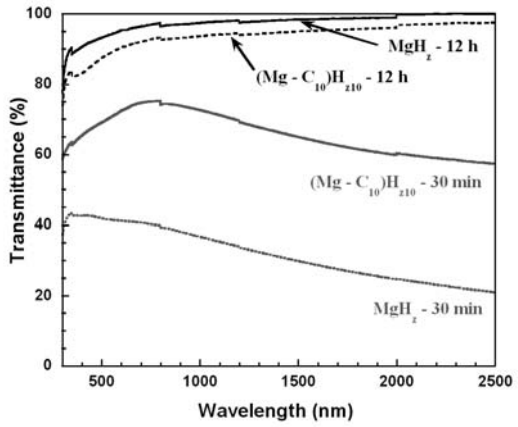

FIGURE 3 : Evolution of the optical transmittance versus the annealing time, under pure H_2 (P(H2)=15 bar) at 200 °C, for MgH and (Mg-C_{10})H thin films, grown on a glass substrate at room temperature in vacuum (10-mbar) and annealed under hydrogen during 30 min and 12 For simplicity, the hydrogen contents being unknown (i.e. unknown Mg/MgH_2 ratio) *ex situ* hydrogenated films are described by (Mg-C)H (x equal to the amount of the carbon inside the target).

C - FeF thin films : Key role of the substrate temperature

The XRD profile of iron fluoride thin film deposited from a FeF_3 target at a 600 °C sub strate temperature corresponds to the well crystallized tetragonal FeF_2 phase (S.G. $P4_2/mnm$) (Fig. 4). The signature of the FeF_3

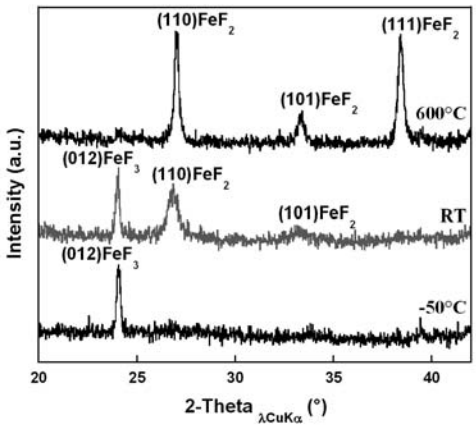

FIGURE 4 : XRD patterns of iron fluoride thin films deposited on stainless steel substrates from FeF3 target in vacuum of 5. 10^{-7} mbar at substrate temperatures of 600 °C, RT, and -50 °c for 1 h at a repetition rate of 10 Hz. Indexing were given by assuming a tetragonal lattice of FeF_2 (S.G. : $P4_2/mnm$) and/or a rhombohedral lattice of FeF_3 (S.G. : $R\bar{3}c$) in hexagonal setting.

deposition pressure, namely 5.10^{-1} mbar, prevents from observing any small pressure fluctuations upon deposition. Therefore, from our various observations, the carbon can simply be described as an oxygen trap.

In agreement with a smaller oxygen contamination, the carbon presence speeds up the hydrogenation process (Fig. 3). After 30 mins of annealing, *ex situ* hydrogenated Mg films show a smaller optical transmittance than the (Mg-Cio) ones (T(MgH_z)≈40%<T((MgC 1o)H1o) 75% at 700 nm). After 12 h of hydrogenation, both films without and with carbon show very close transmittance values (T≈90 %) with even a slightly smaller value for the film containing carbon correlated to absorption phenomena.

phase, represented by the single (012) peak (S.G. : $R\bar{3}c$), appears with decreasing sub strate temperature (≤400 °C [12]) and becomes clearly visible for a RT substrate. At this substrate temperature, the sharpness of the $(0l2)_{FeF3}$ peak is opposed to the broadness of the $(110)_{FeF2}$ one indicating higher crystallinity for the FeF_3 phase compared with the FeF_2 one. Using Scherrer's

formula, average crystallite sizes of 39 and 15 nm were calculated for FeF_3 and FeF_2 phases, respectively [13]. Attempts at isolating the FeF_3 phase by decreasing the laser energy, increasing the deposition rate, increasing the fluorine content inside the target (mixture of XeF_2/FeF_3 target) remains unsuccessful. On the contrary, thanks to our own home made low temperature set up, we observed a progressive and full disappearance of

the $(110)_{FeF2}$ XRD peak with decreasing temperature. Finally for a substrate temperature as low as -50°c, the $(0l2)_{FeF3}$ peak remains as a single peak suggesting at first sight the stabilization of the FeF_3 phase. Surprisingly, in similar deposition conditions, complementary HRTEM and Môssbauer experiments report the co-existence of poorly crystallized FeF_3 phase together with well crystallized FeF_2 phase.

Up to now, the origin of such discrepancy between the XRD and the HRTEM /Môssbauer results are unclear.
for the -50 °C film a short plateau is observed at 1.9 V (Fig. 5). This plateau progressively diseappears upon cycling to become inexistent after 10 cycles. The origin of such a plateau as well as the mechanism associated with the cycling behavior are currently under investigation and will be reported in a forthcoming paper.

IV. CONCLUSION

In this paper, via examples taken in the field of energy storage and conversion, we showed how by playing with the composition, the substrate temperature and the pressure one can control and optimize the thin film growth using the Pulsed Laser Deposition technique. Thanks to M addition, higher cycling life was reported for electrochromic Ni-M-O (M=Ta (10 %), W (5 %)) thin films cycled in KOH electrolyte. *In situ* optical changes from shiny metallic to fully transparent were simply achieved by modifying the pressure of deposition of Mg-based thin films whereas their *ex situ* hydrogenation was facilitated by carbon addition. Finally, the benefit of enlarging substrate temperatures to negative values was illustrated through the example of FeF_x thin films, for which the sub strate temperature is a key factor governing the FeF_2 or/and FeF_3 phase deposition.

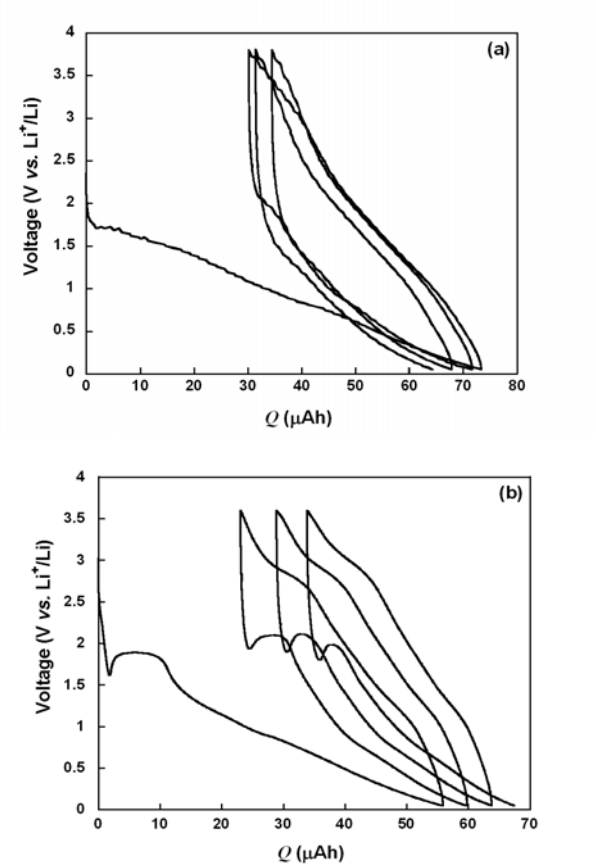

FIGURE 5 : Discharge and charge curves of lithium cells with iron fluoride thin films operated in a voltage window of 0.05-3.60 (or 3.80) V at a 2.8 μA cm^{-2} current density at 25 °C. Thin films were deposited on stainless steel substrates from FeF_3 target in vacuum (a) at 600 °C for 1 h at a repetition rate of 2 Hz with a laser energy of 180 mJ or (b) at -50 °C for 10 min at a repetition rate of 10 Hz with a laser energy of 120 mJ. The electrolyte used was 1 M LiPF6 dissolved in EC/DMC solution (1/1 by volume).

[1] J. Cheung and J. Horwitz, Mat. Res. Soc. *Bull*., 1992.
[2] D.B. Chrisey and G.K. Hubler : Pulsed Laser Deposition of thin films, (Wiley, New York 1994).
[3] V. Pralong, J-B. Leriche, B. Beaudoin, E. Naudin, M. Morcrette and J-M.Tarascon, Solid State Ionics 166 (3/4) 295 (2004).
[4] C. Marcel, M.S. Hegde, A. Rougier, C. Maugy, C. Guéry and J-M. Tarascon, Electrochim. Acta 46(13-14) 2097 (2001).
[5] A. Rougier, F. Portemer, A. Quédé and M. ElMarssi, Appi. Suil Sci. 153 1 (1999).
[6] T.J. Richardson, J.L. Slack, R.D. Armitage, R. Kotescki, B. Frangis and M.D. Rubin, Appi. Phys. Lett. 78 3047 (2001).
[7] J. Isidorsson, lAME. Giebels, E.S. Kooji, N.J. Koerman, J.H. Rector, A.T.M. Van Gogh

and R. Griessen, J. Alloys Compds. 330-332 875 (2002).
[8] N. Penin, A. Rougier, L. Laffont, P. Poizot and J-M. Tarascon, Sol. Energy Mater. Sol. CelIs (in press).
[9] Y. Makimura, A. Rougier and J-M. Tarascon, AppI. S"I Sci. (in press).
[10] A. Rougier, X. Darok, V.V. Bhat, L. Aymard, G.A. Nazri and J-M. Tarascon, Mater. Res. Soc. Froc. Vol. (in press).
[11] R. Janot, L. Aymard, A. Rougier, G.A. Nazri and J-M. Tarascon, J. Mater. Res. Soc. 18(8) 1749 (2003).
[12] Y. Makimura, A. Rougier and J-M. Tarascon, AppI. Su'i Sci. (in press).
[13] P. Scherrer, Nachr. Ges. Wiss., G ôttingen 2 98 (1918).